Results: Although the proposed method is applicable to any chaotic system, without loss of generality, the hyperchaotic system in [5] will be used for illustration. Moreover, the *n*-shift cipher in [6] will be chosen as the encryption function. In testing the proposed method, ASCII text and a sound signal will be used and the diagonal elements of the matrix k are all chosen to be –100. In transmitting ASCII text, the input plaintext, the transmitted ciphertext and the recovered plaintext are given as follows:

Input plaintext: Chaotic synchronisation for secure communication

Transmitted ciphertext:
TH"!eT7+yK\Lp5Gv3u9\"WCv1uH@{LQDq1KGYs!Hq}R3HqR1

Recovered plaintext: Chaotic synchronisation for secure communication.

In the case of transmitting a sound signal, Figs. 2 and 3 show the input signal, the transmitted signal and the recovered signal in the time and frequency domains, respectively.

Conclusion: An observer is designed for synchronisation between an encrypter and a decrypter. Based on the synchronisation scheme, a plaintext can then be transmitted and retrieved with extremely high security. Since there are no constraints on the form of the chaos, the proposed method can be applied to any kind of chaotic system. To show the effectiveness of the proposed method, practical results are presented.

Acknowledgments: This work was supported in part by the National Science Council, Taiwan, Republic of China, under grant NSC89-2213-E-224-074.

23 August 2000
Electronics Letters Online No: 20001333
DOI: 10.1049/el:20001333

Chia-Ju Wu (*Department of Electrical Engineering, National Yunlin University of Science and Technology, Touliu, Yunlin 640, Taiwan, Republic of China*)

Yung-Cheng Lee (*Department of Electrical Engineering, National Huwei Institute of Technology, Huwei, Yunlin 632, Taiwan, Republic of China*)

References

1 PECORA, L.M., and CARROLL, T.L.: 'Synchronization in chaotic systems', *Phys. Rev. Lett.*, 1990, **64**, (8), pp. 821–824
2 PECORA, L.M., and CARROLL, T.L.: 'Synchronizing chaotic circuits', *IEEE Trans. Circuits Syst.*, 1991, **38**, (4), pp. 453–456
3 CUOMO, K.M., OPPENHEIM, A.V., and STROGATZ, S.H.: 'Synchronization of Lorenz-based chaotic circuits with applications to communications', *IEEE Trans. Circuits Syst. II: Analog Digit. Signal Process.*, 1993, **40**, (10), pp. 626–633
4 NIJMEIJER, H., and MAREELS, I.M.Y.: 'An observer looks at synchronization', *IEEE Trans. Circuits Syst. I: Fundam. Theory Appl.*, 1997, **44**, (10), pp. 882–890
5 GRASSI, G., and MASCOLO, S.: 'A system theory approach for designing cryptosystems based on hyperchaos', *IEEE Trans. Circuits Syst. I: Fundam. Theory Appl.*, 1999, **46**, (9), pp. 1135–1138
6 YANG, T., WU, C.W., and CHUA, L.O.: 'Cryptography based on chaotic systems', *IEEE Trans. Circuits Syst. I: Fundam. Theory Appl.*, 1997, **44**, (5), pp. 469–472

Theoretical study of method based on ellipsometry for measurement of complex permittivity of materials

F. Sagnard, F. Bentabet and C. Vignat

A new approach, based on ellipsometry and adapted to microwave frequencies, is presented for the *in situ* measurement of the complex permittivity of materials. The work serves to characterise the accuracy and the sensitivity of the method.

Introduction: Non-destructive methods are valuable approaches for the measurement of the dielectric properties of materials. In the context of indoor wireless communications, free-space methods appear of particular interest for the characterisation and performance prediction of indoor channels, since the measurements are to be carried out on site and should not alter the material [1, 2].

In this Letter we present a new approach, proposed recently by Stetiu [3], based on microwave ellipsometry. This method consists of measuring the depolarisation induced by the reflection of an incident electric field on the surface of the material under test. The principal contribution of our work is to have established that the relative complex permittivity $\tilde{\varepsilon}$ of the material can be deduced from the variation law of the power of the reflected wave, as a function of the rotation angle A of the receiving antenna. Proper implementation of this method presupposes that the Fresnel conditions are met.

In the Fresnel method, determination of the reflection coefficients for the two perpendicular polarisations is critical in the region of the Brewster angle when dealing only with moduli. This drawback appears not to be the case in our method, since the incidence angle θ_i can be freely chosen.

Finally, we PROVIDE a systematic analysis of the uncertainties involved in the measurement process associated with this method.

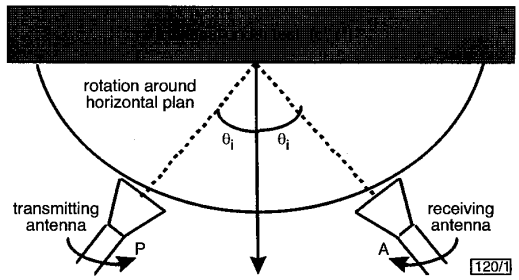

Fig. 1 *Schematic diagram of measurement setup*

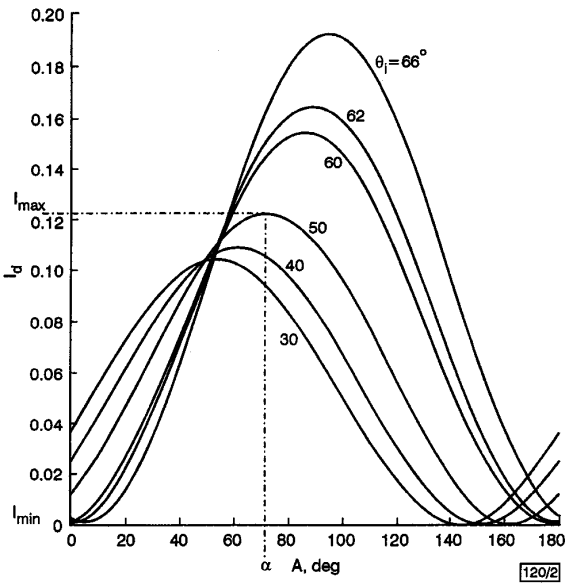

Fig. 2 *Variations of I_d against rotation angle A*

Problem formulation: Fig. 1 shows a schematic diagram of the microwave ellipsometry setup. The transmitting and receiving antennas are rectangular horns that are optimised to radiate a quasi-plane wave-front. This type of horn radiates a linear polarised electric field that becomes elliptically polarised after reflecting on the surface of the material.

The antennas are positioned on a rotation device, the axis of which is horizontal. Choosing a rotation angle $P = -\pi/4$ for the transmitting antenna and considering an incident angle θ_i, the electromagnetic power measured by the receiving antenna expressed as a function of its rotation angle A is [4]:

$$I_d = I[1 - \cos(2A)\cos(2\psi_r) + \sin(2A)\sin(2\psi_r)\cos(\Delta_r)] \quad (1)$$

To eliminate the propagation losses, we subtract, from the detected power, the power involved in the line-of-sight configuration. To deduce the complex permittivity of the material, parameters ψ_r and Δ_r have to be determined. These relate to the reflection coefficients for the parallel and perpendicular polarisation of the electric field $\tilde{r}_p$ and $\tilde{r}_s$, respectively, which in turn depend on the incidence angle θ_i according to

$$\frac{\tilde{r}_p}{\tilde{r}_s} = \tan(\psi_r)e^{j\Delta_r} \quad (2)$$

The expression of intensity I is given by

$$I = \frac{E^2}{4\cos^2\psi_r}|r_s|^2 \quad (3)$$

This variation of intensity I_d against A is shown in Fig. 2 (which, in the case of a concrete wall with permittivity measured at 10GHz, is $\tilde{\varepsilon} = 3.5 - j$, with an incidence angle $\theta_i = 50°$).

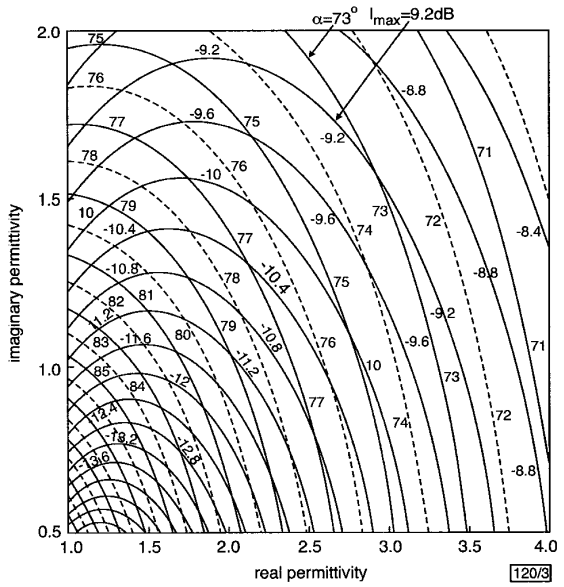

Fig. 3 *Constant value lines of* α *and* I_{max}

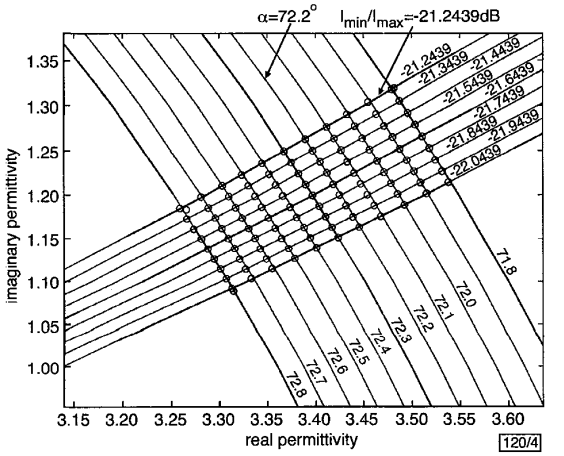

Fig. 4 *Constant value lines of* α *and* $(I_{min}/I_{max})_{dB}$

From the determination of the ratio I_{min}/I_{max} of extremal values of I_d, the excentricity b/a of the ellipse of the electric field can be computed as

$$\tan\chi = \frac{b}{a} = \sqrt{\frac{I_{min}}{I_{max}}} \quad (4)$$

Parameters ψ_r and Δ_r can then be deduced from the knowledge of angle α (corresponding to the maximal intensity) according to the fundamental relations of ellipsometry:

$$\tan 2\alpha = \tan 2\psi_r \cos\Delta_r \quad (5)$$

$$\sin 2\chi = \sin 2\psi_r \sin\Delta_r \quad (6)$$

The sets of constant-$(I_{min}/I_{max})_{dB}$ and constant-α contour lines plotted in the $(\varepsilon', \varepsilon'')$ plane, see Fig. 4, represent a convenient approach for the estimation of the unknown real and imaginary permittivities. This device allows the consequence of a ±0.4dB uncertainty on I_{max} and I_{min}, and of ±0.5° on angle A (maximal uncertainty values compatible with our experimental device) to be evaluated. All the possible values of permittivity fill a parallelogram as shown in Fig. 4 (for $\tilde{\varepsilon} = 3.5 - j$ and a large thickness material, we have $\Delta\varepsilon' = 0.31$ and $\Delta\varepsilon'' = 0.28$).

Proposed method for determining $\tilde{\varepsilon}$*:* In the case of large thickness materials, an analytical expression for $\tilde{\varepsilon}$ can be derived in terms of ψ_r and Δ_r. However, this expression becomes too complex in the case of a layered material: thus, we propose in the following a numerical approach for determining $\tilde{\varepsilon}$. This approach is based on the sole measurement of the extremal values I_{max} and I_{min} of the intensity. However, in practice, I_{min} often takes small values (especially when the relative imaginary permittivity is less than 3 and the incident power is weak), which implies uncertainty relating to the measurement. To eliminate this drawback, we propose an approach comprising the following steps:

(i) the measured values of I_{max} and α and a contour lines chart are used to provide a first guess $\tilde{\varepsilon}_0 = (\varepsilon_0', \varepsilon_0'')$ of the permittivities (Fig. 3)

(ii) the I_{min} value is extracted from the theoretical curve $I_d = f(A)$ associated with $\tilde{\varepsilon}_0$

(iii) couples of real and imaginary permittivities $(\varepsilon', \varepsilon'')$ are regularly sampled in the uncertain parallelepipedic area centred on $\tilde{\varepsilon}_0$

(iv) to each couple of this area, a corresponding characteristic $I_d = F(A)$ is associated (Fig. 4)

(v) the best characteristic is retained as that best fitting the experimental data points, according to a least square criterion

(vi) optimal values $(\varepsilon', \varepsilon'')$ are inferred as the couple corresponding to this best characteristic.

Influence of measurement uncertainties: The influence of measurement errors on parameters θ_i, α and I_{max} can be characterised as follows:

(*a*) A suitable incidence angle θ_i can be chosen so as to minimise the influence of $\Delta\theta_i$ on parameters α and I_{max}; indeed, theoretical plots of the characteristics $\alpha(\theta_i)$ and $I_{max}(\theta_i)$ show both a linear variation against θ_i of around $\theta_i = 45°$, which should thus be adopted for further measurements (Fig. 2).

(*b*) The influence of measurement errors on α and I_{max} on the determination of ε' was studied by plotting the characteristics $\varepsilon'(\alpha)$ and $\varepsilon'(I_{max})$. It can be shown that ε' decreases as α and/or I_{min}/I_{max} decrease. Thus, greater measurement uncertainty is to be expected in the case of larger values of ε', e.g. considering only intensity uncertainties (with $\varepsilon'' = 1$), if $\varepsilon' = 3.5$ and $\varepsilon' = 7$ the uncertainty $\Delta\varepsilon'/\varepsilon'$ can be evaluated to 17.5 and 24.5%, respectively.

(*c*) We have shown that the same variations on α and I_{max} act in the opposite way on the parameter ε''; thus, unlike ε', relative errors are minimised for increasing values of ε'' (greater than 1) but they are more important than in the case of parameter ε', e.g. considering only intensity uncertainties (with $\varepsilon' = 3.5$), if $\varepsilon'' = 2$ and $\varepsilon'' = 3.5$ the uncertainty $\Delta\varepsilon''/\varepsilon''$ can be evaluated to 41.1 and 28.5%, respectively.

Conclusion: In this Letter, we have presented the principles of the microwave ellipsometry method to determine the complex permittivity of materials *in situ*. We have studied its performance for a homogeneous material of large thickness. Consideration of single and double layer materials is currently under study. Measurements will be performed to validate the method and to contrast the results with those obtained by the Fresnel method.

10 July 2000
Electronics Letters Online No: 20001313
DOI: 10.1049/el:20001313

F. Sagnard, F. Bentabet and C. Vignat (*Laboratoire Systèmes de Communication, Cité Descartes, 5, Bd Descartes, Champs-sur-Marne, 77454 Marne-La-Vallée cedex 02, France*)

E-mail: sagnard@univ-mlv.fr

References

1 UMARI, M.H., GHODGAONKAR, D.K., VARADAN, V.V., and VARADAN, V.K.: 'A free space bistatic calibration technique for the measurement of parallel and perpendicular reflection coefficients of planar samples', *IEEE Trans. Instrum. Meas.*, 1991, **40**, (1), pp. 19–24

2 LANDRON, O., FEUERSTEIN, M.J., and RAPPAPORT, T.S.: 'In situ microwave reflection coefficient measurements for smooth and rough exterior wall surfaces'. 43rd Conf. Vehicular Technology, 1993, pp. 77–80

3 STETIU, P., and HANNOVER, B.: 'Ellipsométrie en microondes'. Journées Caractérisation Microondes et Matériaux, La Defense, France, March 2000

4 BORN, M., and WOLF, E.: 'Principles of optics' (Pergamon Press, 1980, 6th edn.)

Ion exchanged waveguide in new active and photosensitive glass

G. Perrone, A. Moro, C. Contardi and D. Milanese

Active channel waveguides have been fabricated by ion exchange in a new erbium-doped, germano-silicate photosensitive glass. The passive and active properties of the waveguides have been investigated by standard techniques.

Introduction: Active glasses are very promising substrates to produce low-cost integrated laser sources, amplifiers and zero-loss components for optical communication systems. Although many combinations of hosts (silicate, phosphates, etc.) and rare earth doping ions (Er, Nd, Pr, etc.) have been proposed in the literature and some of them are already commercially available, new compositions are always sought to further improve the performances.

Some glasses exhibit also photosensitivity, and this is an interesting property since it allows the transfer of the excellent results obtained with fibre based grating assisted devices to similar planar integrated structures to achieve compactness and better mechanical stability. In this framework, we have already reported the synthesis of a new photosensitive ion-exchangeable silicate glass for integrated optics that has been called SGBN from the initials of its main components: oxides of silicon, germanium, boron and sodium. Although a wide range of Ge content is possible, the best results in terms of stability and photosensitivity (maximum induced index variation in the order of 10^{-3} without hydrogen loading) have been obtained for the glass containing 10% wt. of Ge oxide [1].

Recently, we have also reported the synthesis of the first glass family that is at the same time photosensitive, ion-exchangeable and active, by doping the passive SGBN glass with rare earth ions [2]. In this Letter we report the fabrication of channel waveguides by $K^+ \rightarrow Na^+$ ion exchange in the Er-doped SGBN glass and their characterisation in terms of passive and active properties in the third optical communication window.

Glass preparation and waveguide fabrication: The Er-SGBN glass is prepared following the same procedure developed for the passive SGBN glass, i.e. melting extremely high purity oxides and carbonates in platinum crucibles at 1650°C for two hours in air [2]. The melt is stirred using a pure silica mixer and then the most homogeneous batch is extracted by drilling after an annealing lasting up to 13 hours at 550°C to reduce the residual stresses and ensure the necessary mechanical stability. The glass is then characterised from a chemical and physical point of view according to standard techniques such as heating stage microscopy, differential scanning calorimetry (DSC) and compositional analysis (ICP-AES) [2]. As confirmed by DSC measurements, the SGBN is a very promising glass host because it does not show crystallisation onsets within a wide range of Ge and Er concentrations.

The focus of this Letter is the feasibility of the active channel waveguides in the SGBN32, a glass containing 10% wt. GeO_2 and 1% wt. Er_2O_3.

Having a new substrate, to design channel waveguides, it is necessary to determine first the ion exchange characteristic parameters such as the diffusion rate and the maximum index variation. These parameters have been extracted from the characterisation of surface planar slab waveguides fabricated by immersion of the samples in a pure potassium nitrate melt at a temperature of 400°C for different times up to 300 minutes. Applying an inverse WKB method [3] to the modal effective indexes measured with the prism coupling technique, it is possible to fit the recovered index profile with a Gaussian function in the form

$$n(x) = n_b + \Delta n \exp\left[-\left(\frac{x}{d}\right)^2\right]$$

where n_b is the substrate refractive index (bulk), Δn is the surface maximum index variation, and $d = k\sqrt{(D_e t)}$ is the diffusion depth that can be written as a function of the diffusion rate D_e, of the exchange duration t and of a proper constant k. In our case the recovered index parameters are $n_b = 1.521 \pm 0.001$, $\Delta n = 0.0081 \pm 0.0002$, $D_e = (0.15 \pm 0.01)\mu m^2/min$, $k = 2.1$. Their knowledge, together with a suitable modelling of the exchange process, allows the design of any type of surface or buried waveguide device. In particular, we designed a set of surface channel waveguides having widths ranging from 3 to 6μm and supporting a single mode at $\lambda = 1550nm$. These waveguides have been patterned on an aluminium layer, previously evaporated on the surface, using a standard photolithographic technique. Then the ion exchange process has been carried on in the same conditions of the planar samples for 45 minutes.

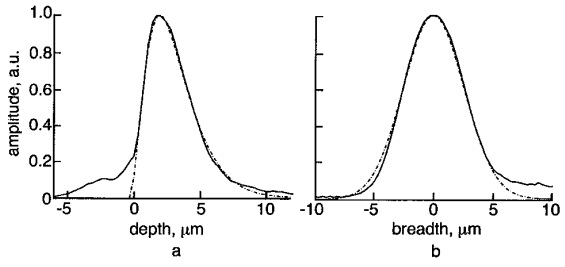

Fig. 1 *Comparison of measured and computed field amplitudes for channel waveguide at signal wavelength*

a Depth cut
b Breadth cut
——— measured
– · – · computed

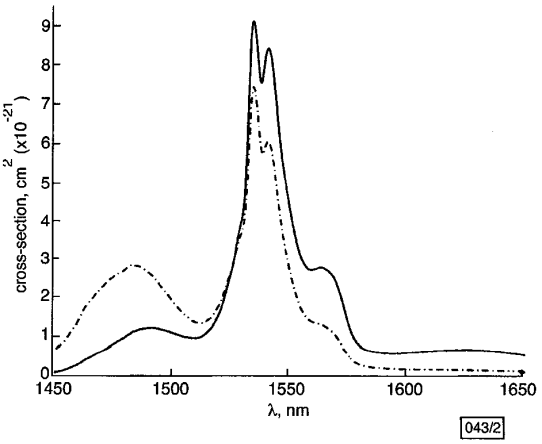

Fig. 2 *Absorption and emission cross-sections for SGBN32 glass*

– · – · absorption
——— emission